

NICMOS spectroscopy of HD 189733b

Mark R. Swain¹, Pieter Deroo¹ and Gautam Vasisht¹

¹Jet Propulsion Laboratory, California Institute of Technology, 4800 Oak Grove, Pasadena, California, 91109, United States
email: Mark.R.Swain@jpl.nasa.gov

Abstract. Spectral features corresponding to methane and water opacity were reported based on transmission spectroscopy of HD 189733b with Hubble/NICMOS. Recently, these data, and a similar data set for XO-1b, have been reexamined in Gibson *et al.* (2010), who claim they cannot reliably reproduce prior results. We examine the methods used by the Gibson team and identify two specific issues that could act to increase the formal uncertainties and to create instability in the minimization process. This would also be consistent with the GPA10 finding that they could not identify a way to select among the several instrument models they constructed. In the case of XO-1b, the Gibson team significantly changed the way in which the instrument model is defined (both with respect to the three approaches they used for HD 189733b, and the approach used by previous authors); this change, which omits the effect of the spectrum position on the detector, makes direct intercomparison of results difficult. In the experience of our group, the position of the spectrum on the detector is an important element of the instrument model because of the significant residual structure in the NICMOS spectral flat field. The approach of changing instrument models significantly complicates understanding the data reduction process and interpreting the results. Our team favors establishing a consistent method of handling NICMOS instrument systematic errors and applying it uniformly to data sets.

Keywords. techniques: spectroscopic, infrared: stars, planetary systems

1. Introduction

Measurements with the NICMOS instrument on the Hubble space telescope demonstrated that molecular spectroscopy of exoplanet atmospheres was possible and provided the first detection of methane in a planet orbiting another star (Swain *et al.* 2008). From this initial result, molecular spectroscopy of exoplanet atmospheres has grown rapidly, using Spitzer (Grillmair *et al.* 2008), Hubble (Swain *et al.* 2009a, 2009b), and ground-based measurements (Swain *et al.* 2010; Thatte *et al.* 2010; Snellen *et al.* 2010). The alkali element sodium has also been detected in exoplanet atmospheres using Hubble, (Charbonneau *et al.* 2002) and ground-based measurements have also been made (Redfield *et al.* 2008; Snellen *et al.* 2008). Spectroscopic measurements reporting an absence of atomic or molecular features have also been reported (Pont *et al.* 2008, 2009), with useful constraints being placed by the measurements. At the present time, numerous teams have exoplanet spectroscopy programs in place, and at least one purpose-built instrument is being constructed (Jurgenson *et al.* 2010). In short, the era of exoplanet characterization via spectroscopy is at hand.

Although the exoplanet spectroscopy field is broadening rapidly, the role of measurements with Hubble/NICMOS is currently unique. Operating in the near-IR, HST/NICMOS has produced published observations of four exoplanet systems, and molecules were detected in three; transmission and emission spectra were obtained, and the measurements show that water, methane, and carbon dioxide are routinely present

in hot-Jupiter atmospheres. Simply put, HST/NICMOS has made an enormous contribution to the area of exoplanet spectroscopy; the fact that the NICMOS instrument is currently not available, with no specific plans to return it to operation, is certainly a setback for the exoplanet community. Given the large and unique impact of the NICMOS instrument, independent confirmation of results is a high priority.

In the recent paper by Gibson, Pont & Aigrain (2010; hereafter GPA10), the authors reanalyzed transmission spectroscopic measurements of HD 189733b (Swain, Vasisht & Tinetti 2008; hereafter SVT08), and XO-1b (Tinetti *et al.* 2010) and find that they cannot reliably reproduce the previous results. Here we explore the differences in method that lead the two teams to such different conclusions.

2. Observations & Methods

The observational scheme for NICMOS exoplanet spectroscopy consists of a series of spectrophotometric observations, $F(t)$, centered on the exoplanet eclipse. For a transmission spectrum, a transit of the planet is observed, and by measuring the difference between in and out-of-eclipse (through modeling with a theoretical light-curve), the exoplanet spectrum is measured. For HD 189733b, two Hubble orbits prior to the transit and two orbits after the transit are observed to establish the out-of-eclipse baseline. For XO-1b, two orbits before and one after transit are observed.

The Hubble/NICMOS instrument introduces systematic effects and the most significant of these are non-random changes in the location of the spectrum with respect to the focal plane array (FPA) pixel grid; the changes, caused by both displacement and

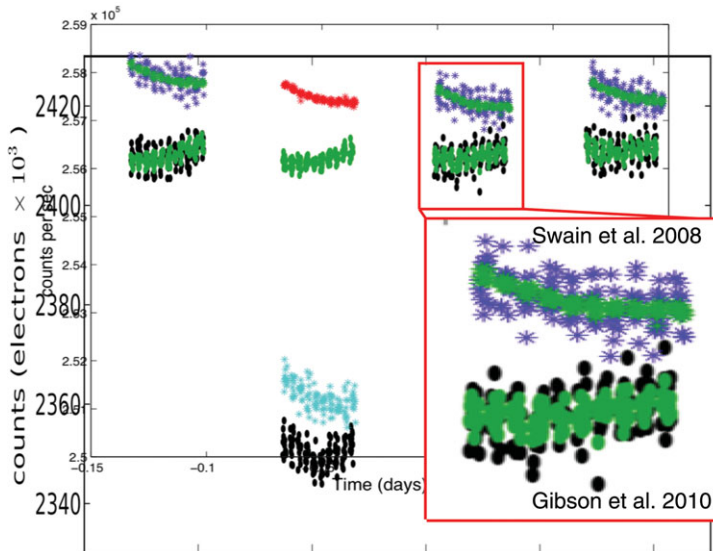


Figure 1. Comparison of the instrument model in SVT08 and GPA10. This figure is the combination of Figure 7 in GPA10 and Figure 7 in the supplementary index of SVT08 over-plotted and rescaled to the same range (the scaling is such that the depth of the primary eclipse is the same). In the inset, we zoom to compare the instrument model of SVT08 and GPA10, which is shown in green in both publications. While the photometry in GPA10 and SVT08 both show similar scatter, the model for the instrument systematic effect in GPA10 is > 3 times larger scatter than the model of SVT08. The large scatter may indicate a poorly determined instrument model that may be factor in producing both the larger uncertainty and decorrelation instability reported by GPA10.

change in the shape of the point spread function, interact with the residual uncertainty ($\sim 5\%$) in the NICMOS FPA flat field. If uncorrected, these systematic errors limit NICMOS spectro-photometry to about 1000 ppm per spectral channel (in the defocused mode used for exoplanet observations). These systematic errors can be corrected using an instrument model to separate instrument effects from astrophysical modulation of the spectrophotometric time series. Our approach is to use linear models because squared terms amplify the noise and reduce the dynamic range of a measurement; if a measurement m is composed of $m = a + b$ where a is the real signal and b is a noise term, $[a + b]^2 \neq a^2 + b^2$. To insure a linear approximation is a valid model, we restrict our analysis to data that have relatively small changes ($\leq 2\%$ of the size of the box used to capture the PSF) in the shift in the position of the spectrum, and we have tested this validity domain both by simulations (synthetic illumination of an actual NICMOS flat field) and real data.

The instrument model we use is constructed from seven instrument state vectors, collectively identified as Ψ_i , where the index i identifies the individual state vectors, which are x position, y position, the angle of the spectrum on the detector, the full width at half maximum of the PSF, the Hubble telescope orbital phase, the orbital phase squared (the error in the quantity is minimal so we admit it as a squared term), and the FPA temperature. With these state vectors, the observed spectrophotometry is modeled using (1) an instrument model constructed using a linear combination of the state vectors, and (2) a light curve model with the radius ratio between planet and star as a free parameter. In SVT08, the two components of the spectrophotometric model are determined separately by establishing the instrument model using the out-of-eclipse data and then applying the interpolated model to the in-eclipse portion of the light curve. For XO-1b in Tinetti *et al.* (2010), both components are determined simultaneously through a joint minimization over the entire time-domain (including in-eclipse). This calibration approach has been described in detail in SVT08 and updated in Swain *et al.* (2009, 2009b). The minimization process minimizes the residual ϵ obtained by removing the eclipse light curve and the instrument model from the data:

$$\epsilon(t) = F(t) - LM(d, t) \times \sum_i \beta_i \dot{\Psi}_i(t) \quad (2.1)$$

where the β_i are the model coefficients for the instrument state vectors, and d is the eclipse depth parameter for an idealized light curve model LM , which includes limb darkening. The minimization is done using either the Gauss-Markov method (SVT08) or using a downhill simplex method (for joint minimization; Tinetti *et al.* 2010), with both methods producing statistically identical results. This approach produces an exoplanet spectrum by estimating the eclipse depth at every wavelength, and the error bars are determined by the fit residuals and full monte-carlo simulations for error propagation.

3. Discussion

The GPA10 approach differs significantly from the SVT08 approach, and this complicates comparing the methods in detail. The first major difference is the use by GPA10 of multiple instrument models; state vectors are sometimes included, sometimes excluded, and sometimes included as squared terms. The second major difference is the use of a residual permutation algorithm (RPA), which GPA10 uses to feed back permuted, post-decorrelated residuals into the predecorrelated light curve. Use of the RPA in this manner (the feedback step), prior to application of all systematic error removal steps, will inject

noise power from an otherwise correctable systematic error into the light-curve parameter determination. It appears that GPA10 did apply the RPA approach prior to correcting the 'channel-to-channel' variations (SVT08), which have also been termed 'gain-like' variations Burke *et al.* 2010. This could contribute to the larger uncertainties in the GPA10 analysis.

There is one aspect of the GPA10 and SVT08 methods that appears to be directly comparable; this is the comparison of one particular instantiation of the GPA10 instrument models and the instrument model from SVT08. For clarity, we will term this model GPA_189_m1 as it differs substantially from two other instrument models, GPA_189_m2 and GPA_189_m3, that GPA10 also discuss. GPA_189_m1 is defined using the same state vectors as SVT08, and Fig. 1 shows a direct comparison of the SVT08 and the GPA_189_m1 instrument models. The comparison shows that the GPA_189_m1 instrument model has an internal scatter that is ~ 3 times larger than the internal scatter of the SVT08 instrument model. This cannot be the result of worse photon noise in GPA10; based on the number of electrons and taking into account the analog-digital conversion gain of 6.5 (electrons/DN), the photon noise of the GPA10 photometry should be 20% better than the photon noise % in the SVT08 model. A possible explanation for the increased scatter in the GPA10_189_m1 instrument model could be a poorly determined state vector; reprocessing the original SVT08 data set with our group's current pipeline (the original scripts are missing) suggests that the angle vector determination might be a contributor to the difference between the GPA10_189_m1 instrument model and the SVT08 instrument model. However, this is only a suggestion, and a detailed comparison of both the instrument state vectors and the model coefficients would be necessary to establish a clear causal connection. Regardless of the origin, the larger scatter in the GPA10_189_m1 instrument model is a possible contributor to larger formal uncertainties in the final spectrum, and we note that the spectrum derived using the GPA10_189_m1 model is reasonably consistent (albeit with larger errors) with the SVT08 result.

An interesting question to consider is the possible effects of larger uncertainties in model selection and in decorrelation stability. As discussed above, both (1) the details of the RPA method implementation, and (2) the way in which the instrument models were constructed could act to increase the formal uncertainties in the GPA10 analysis. It is possible that this would have made the decorrelation process sufficiently marginal, by effectively reducing the signal to noise of the data, that it made it difficult for GPA10 to identify a valid instrument model. One indication consistent with this hypothesis is that GPA10 found decorrelation results that were unstable in that the result changed when portions of the data were omitted; this contrasts strongly with the situation SVT08 found, where portions of the data were omitted and the decorrelation results were stable (see SVT08 Supplemental Information).

A detailed comparison of Tinetti *et al.* (2010) results with GPA10 is not really possible because of the radically different instrument model favored by GPA10, which omits the x, y, and angular position information of the spectrum on the detector. We found this change in the definition of the instrument model surprising. In the experience of our group, the position of the spectrum on the detector is an important element of the instrument model because of the significant residual structure in the NICMOS spectral flat field. The instrument model used by GPA10 for XO-1b also differs from the instrument models they constructed for the HD 189733b observations. This approach of constantly changing instrument models, together with the uncertainties in the implementation of the RPA method and in the model determination, makes it very difficult to understand what is going on.

The view in our group is that we employ a consistent instrument model based on the definition in section 2. Using this method, we have published four exoplanet spectra with Hubble/NICMOS data (two transmission spectra and two emission spectra). The method does not work on all Hubble/NICMOS data sets; sometimes there are jumps in the position of the spectrum which are simply too large, and we do not attempt to recover a spectrum in these cases. Our objective for the Hubble/NICMOS measurement has been to enable the process of comparative planetology with near-IR spectra based on a consistent measurement method. In all of the cases where we published Hubble/NICMOS spectra, we tested the stability of the decorrelation by exclusion of some data; this is standard process for our data analysis. In none of these (published) cases did we find a problem with stability of the results. An ideal test of the Hubble/NICMOS results would be confirming observations with a different instrument. Recently reported, ground-based, near-IR emission spectra of HD 189733b (Swain *et al.* 2010; Thatte *et al.* 2010) are consistent with the previous Hubble/NICMOS measurements (Swain *et al.* 2009a); this detection of the same spectral shape by two completely different instruments, with two completely different sets of systematics, is a strong indication that both instruments are measuring the exoplanet emission spectrum.

4. Conclusions

There are several important differences between the approach used by our team and the approach used by GPA10. We have identified two potential ways in which additional noise may be incorporated in the GPA10 calibration process. This additional noise may, in turn, impact the GPA10 decorrelation stability tests and thus some of their conclusions. However, the most significant difference in the approach used by GPA10 and our team may reflect a philosophical difference. GPA10 favor a fundamentally different instrument model for each of the three objects they consider; in contrast, our team has used a single, consistent instrument model for the four reported Hubble/NICMOS spectra. We strongly favor a consistent calibration approach to facilitate intercomparison of exoplanet spectra.

5. Acknowledgements

The research was carried out at the Jet Propulsion Laboratory, California Institute of Technology, under contract with the National Aeronautics and Space Administration.

References

- Burke, C. *et al.* 2010, *ApJ*, 719, 1796
Charbonneau, D., Brown, T. M., & Noyes, R. W., Gilliland R. L. 2002, *ApJ*, 568, 377
Gibson, N. P., Pont, F., & Aigrain, S. 2011, *MNRAS*, 411, 2199
Grillmair, C. J., *et al.* 2008, *Nature*, 456, 767
Jurgenson, C., *et al.* 2010, *SPIE*, 7735, 43J
Pont, F., Knutson, H., Gilliland, R. L., Moutou, C., & Charbonneau, D. 2008, *MNRAS*, 385, 109
Pont, F., Gilliland, R. L., Knutson, H., Holman, M., & Charbonneau, D. 2009, *MNRAS*, 393, 6
Redfield, S., Endl M., Cochran, W. D., & Koesterke, L. 2008, *ApJ* (Letters), 673, 87
Swain, M. R., Vasisht, G., & Tinetti, G.. 2008, *Nature*, 452, 329
Swain, M. R., Vasisht, G., Tinetti, G., Bouwman, J., Chen, P., Yung, Y., Deming, D., & Deroo, P. 2009a, *ApJ* (Letters), 690, 114
Swain, M. R., *et al.* 2009b, *ApJ* (Letters), 704, 1616

Swain, M. R., *et al.* 2010, *Nature*, 463, 637

Snellen, I. A. G., Albrecht, S., De Mooij, E. J. W., & Le Poole, R. S. 2008, *A&A*, 483, 375

Snellen, I. A. G., de Kok, R. J., De Mooij, E. J. W., & Albrecht, S. 2010, *Nature*, 465, 1049

Thatte, A., Deroo, P., & Swain, M. R. 2010, *A&A*, 523, 35

Tinetti, G., Deroo, P., Swain, M. R., Griffith, C. A., Vasisht, G., Brown, L. R., Burke, C., & McCullough, P. 2010, *ApJ* (Letters), 712, 139